SLAC-PUB-1701
January 1976
(T/E)

Amplitudes and Exchange Mechanisms for K*(890) and K*(1420) Production*

P. Estabrooks** and A. D. Martin
Department of Physics
University of Durham
Durham City, England

G. W. Brandenburg†, R. K. Carnegie††, R. J. Cashmore†††, M. Davier‡, W. M. Dunwoodie, T. A. Lasinski, D. W. G. S. Leith, J. A. J. Matthews‡‡, P. Walden‡‡‡, and S. H. Williams

Stanford Linear Accelerator Center
Stanford University, Stanford, California 94305

Abstract:

The $\bar{K}^*(890)$ and $\bar{K}^*(1420)$ production amplitudes are determined using data on the reaction $K^-p \to K^-\pi^+n$ at 13 GeV/c. The energy dependence of $\bar{K}^*(890)$ production is investigated by using in addition the corresponding data at 4 GeV/c. A simple model, based on exchange degenerate Regge poles together with non-evasive 'cut' contributions, is found to provide a good description of all features of the data.

(Submitted to Physics Letters)

*Work supported by the U.K. Science Research Council and the U.S. Energy Research and Development Administration.

Present address:

** Department of Physics, McGill University, Montreal, Quebec, Canada.
† Department of Physics, MIT, Cambridge, Massachusetts.
†† Department of Physics, Carleton University, Ottawa, Ontario, Canada.
††† Department of Physics, Oxofrd University, Keble Road, Oxford, England.
‡ Laboratoire de l'Accelerateur Linéaire, Orsay, France,
‡‡ Department of Physics, Michigan State University, East Lansing, Michigan.
‡‡‡ TRIUMF, University of British Columbia, Vancouver, B.C., Canada.

The high statistics data[1] for the line reversed reactions

$$K^- p \to \bar{K}^{*o}(890)n \qquad (1)$$

$$K^+ n \to K^{*o}(890)p \qquad (2)$$

at 4 GeV/c provide valuable information on the exchange mechanisms for K* production[1,2]. In particular, these data make possible the separation of positive and negative G-parity exchanges. In ref. 2 it was found that the data could be described simply in terms of exchange-degenerate (EXD) Regge poles and non-EXD non-evasive contributions which have equal helicity 1 natural and unnatural parity exchange components in the t channel frame. In this letter we analyse the high statistics data for the reaction $K^- p \to (K^- \pi^+)n$ at 13 GeV/c[3]. The results for reaction (1) at 13 GeV/c, together with those at 4 GeV/c, then enable us to investigate the energy dependence of this reaction. In addition, the higher energy data enable us to determine not only the amplitudes for reaction (1), but also for

$$K^- p \to \bar{K}^{*o}(1420)n \qquad (3)$$

so that we can also study the exchange mechanisms as a function of the mass of the produced $K\pi$ system.

In Fig. 1 we show the 13 GeV/c t channel data for the $K^- p \to K^- \pi^+ n$ partial cross sections

$$\sigma_o \equiv p_L^2(\rho_{oo}+\tfrac{1}{3}\rho_{ss})\frac{d\sigma}{dt}$$

$$\sigma_+ \equiv p_L^2(\rho_{11}+\rho_{1-1}+\tfrac{1}{3}\rho_{ss})\frac{d\sigma}{dt}$$

$$\sigma_- \equiv p_L^2(\rho_{11}-\rho_{1-1}+\tfrac{1}{3}\rho_{ss})\frac{d\sigma}{dt} \qquad (4)$$

in the $\bar{K}^*(890)$ region in comparison with the corresponding data at 4 GeV/c;

p_L is the laboratory momentum of the beam. We have normalized the 13 GeV/c data so that the extrapolated ($t=\mu^2$) value of σ_o is the same at the two energies,† assuming a t-dependence of the form $(-t)\exp(A(t-\mu^2))/(\mu^2-t)^2$. We see that σ_o and σ_- have a somewhat steeper t dependence at 13 GeV/c than at 4 GeV/c and that the natural parity exchange cross section, σ_+, for $-t>0.2$ GeV^2 is a much larger component of $d\sigma/dt$ at 13 GeV/c than at 4 GeV/c. This is more apparent in Fig. 2 where we plot the effective trajectories, $\alpha_{eff}(t)$, obtained from the cross-section components of eqs. (4). The values of α_{eff} for σ_o and σ_- (σ_+) are compared in Fig. 2 with a linear π-B (A_2-ρ) trajectory of slope 0.8 GeV^{-2}.

We now study the amplitudes and exchange mechanisms for $\bar{K}^*(890)$ production at 13 GeV/c. As described in ref. 2, if only S and P wave $K\pi$ production are important, the data yield directly the magnitudes S_o, P_o, $P_\pm$, and the (S_o, P_o) and (P_o, P_-) relative phases. S_o and P_o describe helicity zero $K\pi$ production and, to leading order in the energy, the helicity one amplitude combinations $P_\pm \equiv (P_{\lambda=1} \pm P_{\lambda=-1})/\sqrt{2}$ describe $\bar{K}^*$ production by natural and unnatural parity exchange. The results of such a t independent amplitude analysis of the 13 GeV/c $K^-p \to K^-\pi^+n$ data[3] in the mass region $0.87<M_{K\pi}<0.92$ GeV are shown in Fig. 3. The amplitudes are normalized so that

$$\frac{\Gamma}{\Delta M} p_L^{\,2} \frac{d\sigma}{dt} = \langle \sin^2\delta_p \rangle \left(|P_o|^2+|P_+|^2+|P_-|^2\right) + |S_o|^2 \qquad (5)$$

where the brackets indicate an average over the $K\pi$ mass interval, ΔM.

---

†The $\bar{K}^*(890)$ region is defined by the mass interval $0.87 \leq M(K^-\pi^+) \leq 0.92$ GeV at 13 GeV/c and by $0.84 \leq M(K^-\pi^+) \leq 0.94$ GeV at 4 GeV/c. With this difference taken into account, the extrapolated values of σ_o at the two energies agree within 4%, well within the experimental normalization uncertainty.

We assume that δ_p, the P wave $K\pi$ phase, is given by a K^* Breit-Wigner resonance form [M=893 MeV, Γ=50 MeV, R=5 GeV^{-1} in the notation of ref. 4] and that δ_s is constant across the mass interval. The factor $\Gamma/\Delta M$ is included so that the normalization of $|L_\lambda|^2$ does not depend on the size of the mass interval.

To study exchange mechanisms we recall that the 4 GeV/c ANL data for the line reversed K^* and $\bar{K}^*$ production reactions can be described[2)] simply in terms of the following exchanges

$$\begin{aligned} P_o &= \pi \pm B \\ P_- &= C \pm C' \\ P_+^{\,f} &= C \pm C' + A_2 \pm \rho \end{aligned} \tag{6}$$

together with a nucleon helicity non-flip contribution to the P_+ amplitude which is specified in terms of the A_2,ρ contribution to $P_+^{\,f}$, namely

$$P_+^{\,nf} = \tfrac{1}{4}(A_2 \pm \rho)/\sqrt{-t'} \; . \tag{7}$$

The Regge pole exchanges (π, B), and also (A_2, ρ) are assumed to be (strongly) EXD with a trajectory slope α'=0.8 GeV^{-2}; the (+,-) signs are associated with reactions (2) and (1) respectively. Thus the t dependence of $\bar{K}^*$ production can be parametrized as

$$P_o = g\,\frac{\sqrt{-t}}{\mu^2 - t}\,, \qquad P_- = C_{eff} = g\gamma_c\, e^{b_c(t-\mu^2)}\, e^{i\phi}\,,$$

$$P_+^{\,f} = C_{eff} - i(-t')\, g\gamma_A e^{b_A(t-\mu^2)} \tag{8}$$

where† $g = Ge^{b(t-\mu^2)}e^{i\delta_p^R}$. The factor $-i$ in P_+ occurs because $\alpha_{A_2} - \alpha_\pi$=0.5. We allow for S wave $K\pi$ production under the $\bar{K}^*(890)$ using

$$\frac{S_o}{P_o} = \frac{(\sin\delta_s e^{i\delta_s} + \frac{1}{2}\sin\delta_s^3\, e^{i\delta_s^3})}{\sqrt{3}\quad e^{i\,\delta_p^R}}\; e^{b_s(t-\mu^2)} \tag{9}$$

where b_s and the $I=\frac{1}{2}$ S wave $K\pi$ phase, δ_s, are free parameters, and the $I=\frac{3}{2}$ phase, δ_s^3, is taken[5] to be -10^o.

The curves on Figs. 1 and 3 correspond to this simple parametrization, with parameter values obtained by means of least squares fits to the 13 GeV/c $\bar{K}^*(890)$ data for $-t<0.35$ GeV^2; they are seen to provide a good description of the data and of the amplitudes obtained treating each t bin independently. The values of the parameters are given in the table along with those obtained by means of similar fits to the 4 GeV/c $K^-p\to K^-\pi^+n$ data. The values of G at 4 and 13 GeV/c indicate that the experimental normalizations are in excellent agreement. The variation in the values of b and γ_A in going from 4 to 13 GeV/c is in accord with Regge expectations, and would give $\alpha_\pi'=0.8$ GeV^{-2} and $\alpha_{A_2}-\alpha_\pi=0.8\pm0.2$. Moreover there is good agreement between δ_s at the two energies. For the non-evasive contribution, C_{eff}, the values of γ_c and b_c imply an effective trajectory parallel to, but some 0.15 above, the assumed π-B trajectory.

The simple model described above and in ref. 2 is able to account successfully for the main features of the energy dependence of $\bar{K}^*$ production, as well as of the t dependence of the 4 and 13 GeV/c data. This can also be seen from Fig. 2 where the dashed line corresponds to the $\alpha_{eff}(\sigma_+)$ obtained from the 4 GeV/c amplitude decomposition[2] assuming the A_2-ρ trajectory lies half a unit above the effective trajectory for C_{eff}. The structure in α_{eff} (σ_+) arises because the non-evasive contribution dominates at small $|t|$ whereas A_2-ρ exchange dominates at the larger $|t|$ values. For line-reversed K^* production (reaction (2)) the model[2] predicts the $\alpha_{eff}(\sigma_+)$ shown by the dotted line; the more pronounced structure is due to destructive interference between the A_2-ρ exchange and the non-evasive contributions.

S, P and D wave $K\pi$ spin states. With the assumption of spin coherence at the nucleon vertex, there are thus nine production amplitudes[6] ($S_o, P_o, P_\pm, D_o, D_{1\pm}, D_{2\pm}$) to determine from the 15 measurable moments of the $K\pi$ angular distribution ($\langle Y_M^J \rangle$ with $J \leq 4$, $0 \leq M \leq J$). Fortunately the data suggest simplifications which allow an amplitude analysis to be performed. The moments with $M>2$ in the t channel frame are consistent with zero; this implies $D_{2\pm} \simeq 0$ and so we neglect these amplitudes†. Also the P wave amplitudes are found to be small, as would be expected since the odd J moments are small. A reliable estimation of the magnitudes of S_o, D_o, $D_{1\pm}$ and the (S_o, D_o) and (D_o, D_{1-}) relative phases can therefore be obtained from the seven moments with J even and $M \leq 2$. However, in Fig. 4 we present the results from a more complete analysis which uses all the observed moments (and error correlations) and includes the small P wave contributions. We determine $|P_o|$ and the phase $\Delta_p \equiv \arg(P_o/D_o)$, but we specify $P_\pm$ in terms of $D_{1\pm}$‡

Before comparing the $\bar{K}^*(890)$ and $\bar{K}^*(1420)$ production amplitudes it is useful to fit the data in the $\bar{K}^*(1420)$ mass region in terms of the exchange contributions of eqs.(6). The t dependence of $\bar{K}^*(1420)$ production is parametrized by eqs. (8) with (D_o, $D_{1\pm}$) replacing ($P_o, P_\pm$). The lower partial waves†† are described by relations similar to that implied by eq. (9), namely

$$\frac{S_o}{D_o} = \gamma_s \, e^{i\Delta_s} e^{b_s(t-\mu^2)}, \qquad \frac{P_o}{D_o} = \gamma_p \, e^{i\Delta_p} \tag{10}$$

with $P_\pm$ included as in the t independent analysis. The $\bar{K}^*(1420)$ parameters listed in the table are obtained by fitting to the data for $-t<0.4$ GeV^2.

---

†We present results for data obtained with the $M \geq 3$ moments set to zero.

‡We use the relations $P_\pm = (D_{1\pm}/D_o)P_o/\sqrt{3}$ as expected from absorptive correc-

They provide a good description of the data and agree well with the results of the analysis t bin by t bin as illustrated by the curves on Fig. 4.

The Regge exchange contributions to $\bar{K}^*(890)$ and $\bar{K}^*(1420)$ production can be related by considering duality for Reggeon-particle scattering amplitudes.[7] This approach predicts that the natural parity (A_2-ρ) exchanges should, on average, decrease relative to π-B exchange with increasing $K\pi$ mass as

$$(M_{K\pi}^2)^{\alpha_\pi - \alpha_{A_2}} \sim M_{K\pi}^{-1}$$

From the values of γ_A (and b_A) we see that our $\bar{K}^*(890)$ and $\bar{K}^*(1420)$ amplitude decompositions are consistent with this prediction for $-t \sim 0.3$ GeV^2, where A_2-ρ exchange makes a large contribution to the cross section.

The non-evasive (or 'cut') contributions may be compared with the expectations of the Williams model[8], in which, at small t

$$C_W = -\frac{\sqrt{2}\,M_{K\pi}}{\sqrt{L(L+1)}} \quad \frac{\sqrt{-t}}{\mu^2 - t} \quad \frac{L_{1-}^{(t)}}{L_o^{(t)}} \tag{11}$$

is equal to 1. This model is equivalent to replacing the π pole contribution, $t/(t-\mu^2)$, in the s channel overall non-flip amplitude by $\mu^2/(t-\mu^2)$. At $-t \sim 0.05$ GeV^2, we find C_W=1.12 at 13 GeV/c (C_W=0.96 at 4 GeV/c) for $\bar{K}^*(890)$ production, as compared to $C_W \sim 0.55$ for $\bar{K}^*(1420)$ production (see also ref. 9). This corresponds to a suppression of the 'cut' effect with increasing $M_{K\pi}$. Similar results are found for $\pi\pi$ production where in the ρ region $C_W \sim 1.0$ as compared to $C_W \sim 0.57$ for $f(2^+)$ production[6]. No clear understanding of this suppression exists.

In summary, we have used the high statistics 13 GeV/c $K^- p \to K^- \pi^+ n$ data to determine the $\bar{K}^*(890)$ and $\bar{K}^*(1420)$ production amplitudes. Using the model of ref. 2 based on data[1] for the line reversed reactions, (1), (2), we were able to study both the s and t dependence of the $\bar{K}^*$ production mechanisms. A simple model based on EXD Regge poles together with non-evasive contributions is found to give a good description of all features of the data. Comparing $\bar{K}^*(1420)$ with $\bar{K}^*(890)$ production, we find that the reaction mechanisms have a similar dependence on mass to that found for the SU(3) related $\pi^- p \to \rho n$ and $\pi^- p \to f n$ processes[6].

Acknowledgement

We thank the members of the Argonne EMS group, in particular Barry Wicklund, for the use of their data.

References

1. A. B. Wicklund et al., Argonne National Laboratory report (in preparation); contributed paper to the XVII Int. Conf. on H.E. Physics, London (1974).
2. P. Estabrooks and A. D. Martin, Nucl. Phys. B101, (1975)
3. G. W. Brandenburg, R. K. Carnegie, R. J. Cashmore, M. Davier, W. M. Dunwoodie, T. A. Lasinski, D. W. G. S. Leith, J. A. J. Matthews, P. Walden and S. H. Williams, SLAC-PUB-1641 (1975)
4. P. Estabrooks and A. D. Martin, Nucl. Phys. B79 (1974) 301
5. H. H. Bingham et al., Nucl. Phys. B41 (1972) 1, and references therein
6. A. D. Martin and C. Michael, Nucl. Phys. B84 (1975) 83
7. P. Hoyer and J. Kwiecinski, Nucl. Phys. B60 (1973) 26

   P. Hoyer, R. G. Roberts and D. P. Roy, Nucl. Phys. B56 (1973) 173
8. P. K. Williams, Phys. Rev. D1 (1970) 1312
9. W. Ochs and F. Wagner, Phys. Letts. 44B (1973) 271

Table

	$\bar{K}^*(890)$		$\bar{K}^*(1420)$	
	4 GeV/c	13 GeV/c	13 GeV/c	
G	1.39±0.02	1.42±0.02		1.26±0.04
b	1.5 ±0.1	2.4±0.1		3.2±0.3
γ_c	1.24±0.06	1.46±0.06		0.62±0.07
ϕ	203±6	171±3		196±10
b_c	2.0±0.5	2.1±0.4		-1.0±0.6
γ_A	8.2±1.5	20.6±0.6		4.4±1.0
b_A	2.4±0.6	2.6±0.2		0
δ_s	48±4	41±2	γ_s	1.03±0.09
b_s	4.2±1.4	0.8±0.6	Δ_s	46±4
			b_s	-1.2 ±0.5
			γ_p	0.21±0.07
			Δ_p	73±13

The parameter values obtained in fitting to $K^-p \to K^-\pi^+n$ data using the parametrization of eqs. (8) and (9) or (10). The units are appropriate powers of GeV except for G, which has units of $\sqrt{mb}$ GeV[illegible]. The normalisation is for $\bar{K}^*$ production in the $K^-\pi^+$ mode; the amplitudes should be multiplied by $\sqrt{3/2}$ to account for the $\bar{K}^o\pi^o$ decay mode.

Figure Captions

Fig. 1 The components of the $K^-p\rightarrow\bar{K}^*(890)n$ cross section in the t channel, as defined by eqs. (4), calculated from data at 4 GeV/c and 13 GeV/c. The 13 GeV/c data are normalized so that $\sigma_0(t=\mu^2)$ is equal at the two energies. The curves are obtained from the exchange model of eqs. (6-9) using the parameters listed in the table. (The poor fit of the 4 GeV/c σ_- for $-t>0.2$ is due to a poor description of the large S wave component which dominates σ_- at these t values).

Fig. 2 The values of α_{eff} calculated from the $\bar{K}^*(890)$ data of Fig. 1 using $\sigma\sim s^{2\alpha_{eff}}$, compared with linear Regge trajectories of slope $\alpha'=0.8$ GeV^{-2}. The dashed (dotted) curve is the prediction of the exchange model of ref. 2 for the energy dependence of σ_+ for $\bar{K}^*(K^*)$ production.

Fig. 3 The $\bar{K}^*(890)$ production amplitudes in the t channel frame obtained from the 13 GeV/c $K^-p\rightarrow K^-\pi^+n$ data in the mass interval $0.87<M_{K\pi}<0.92$ GeV. The data for the points with dotted error bars do not satisfy positivity constraints. The curves correspond to the model parametrization described in the text.

Fig. 4 The $\bar{K}^*(1420)$ production amplitudes in the t channel frame obtained from the 13 GeV/c $K^-p\rightarrow K^-\pi^+n$ data in the mass region $1.36<M_{K\pi}<1.48$ GeV. The curves correspond to the model parametrization described in the text.

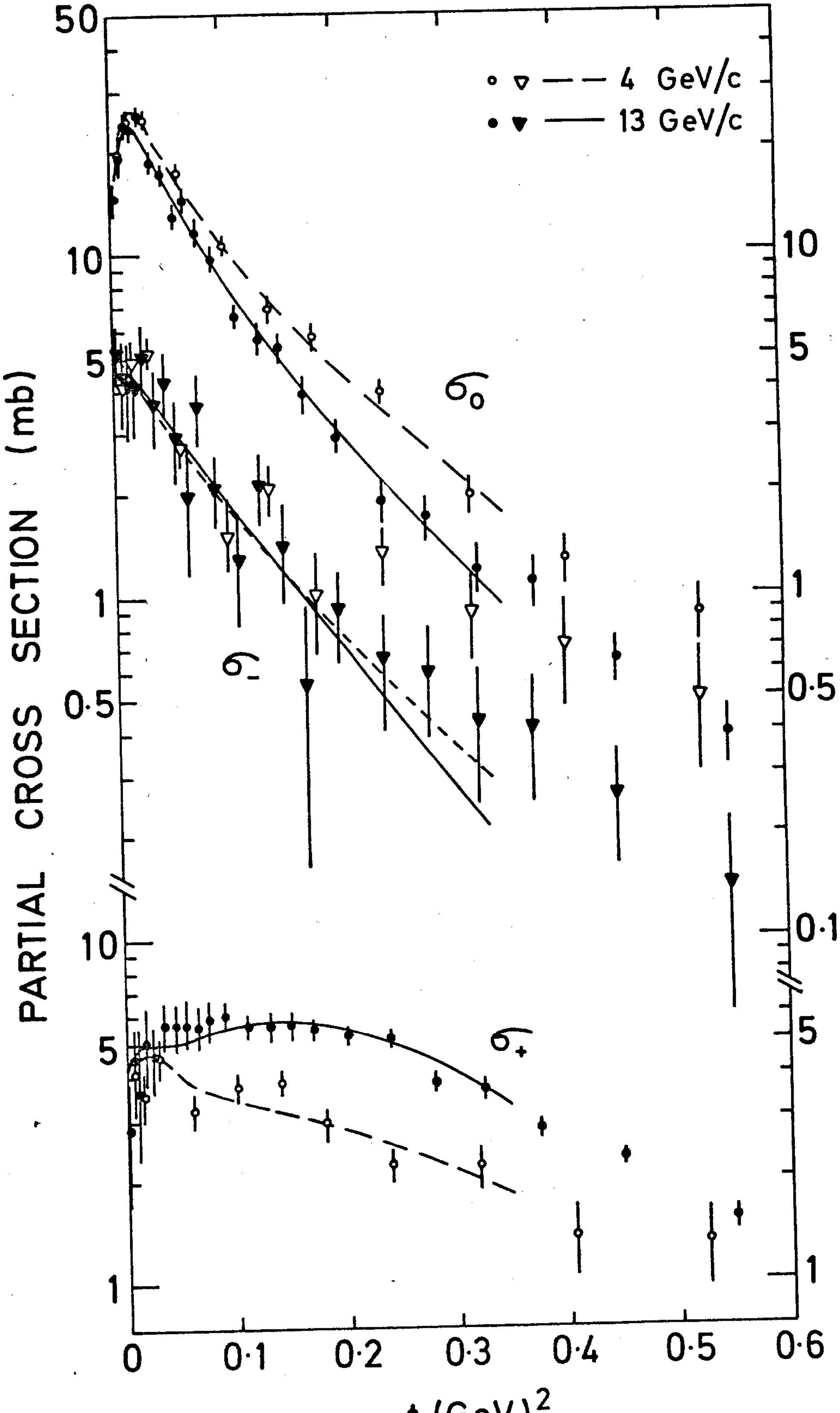

50
10
5
1
0·5
10
5
1
10
5
1
0·5
0·1
5
1
0
0·1
0·2
0·3
0·4
0·5
0·6
-t (GeV)^2
PARTIAL CROSS SECTION (mb)
4 GeV/c
13 GeV/c
σ_0
σ_-
σ_+

FIG. 1.

EFFECTIVE TRAJECTORIES FOR $K^- p \to \bar{K}^*(890) n$

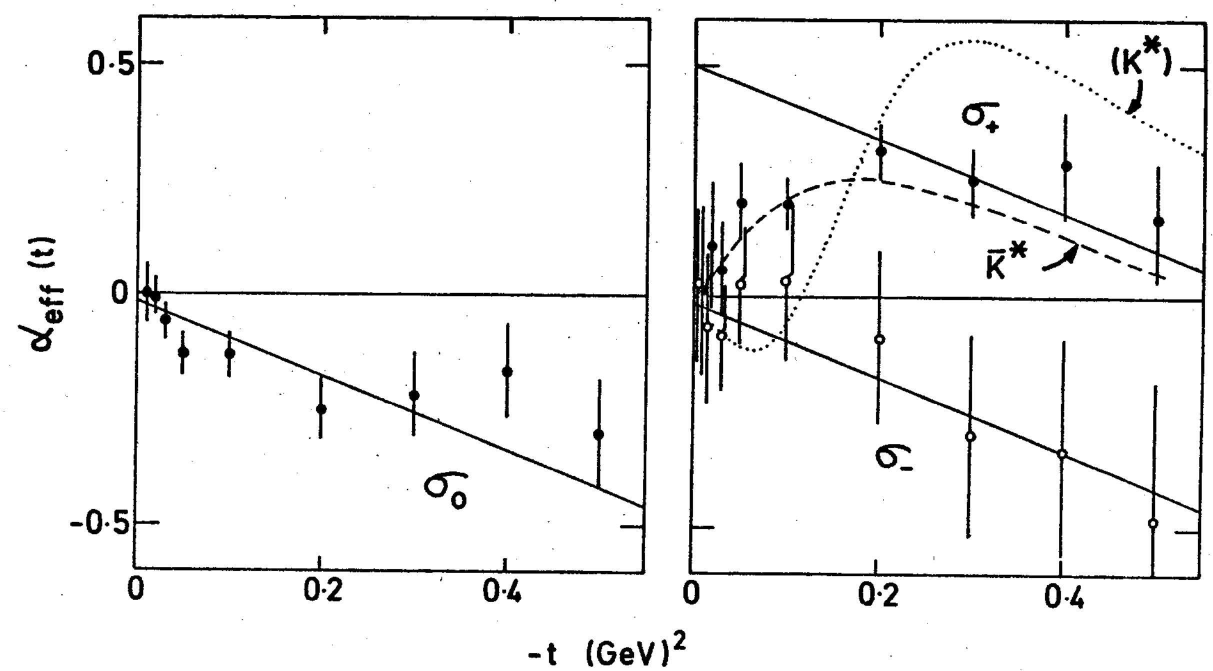

FIG. 2

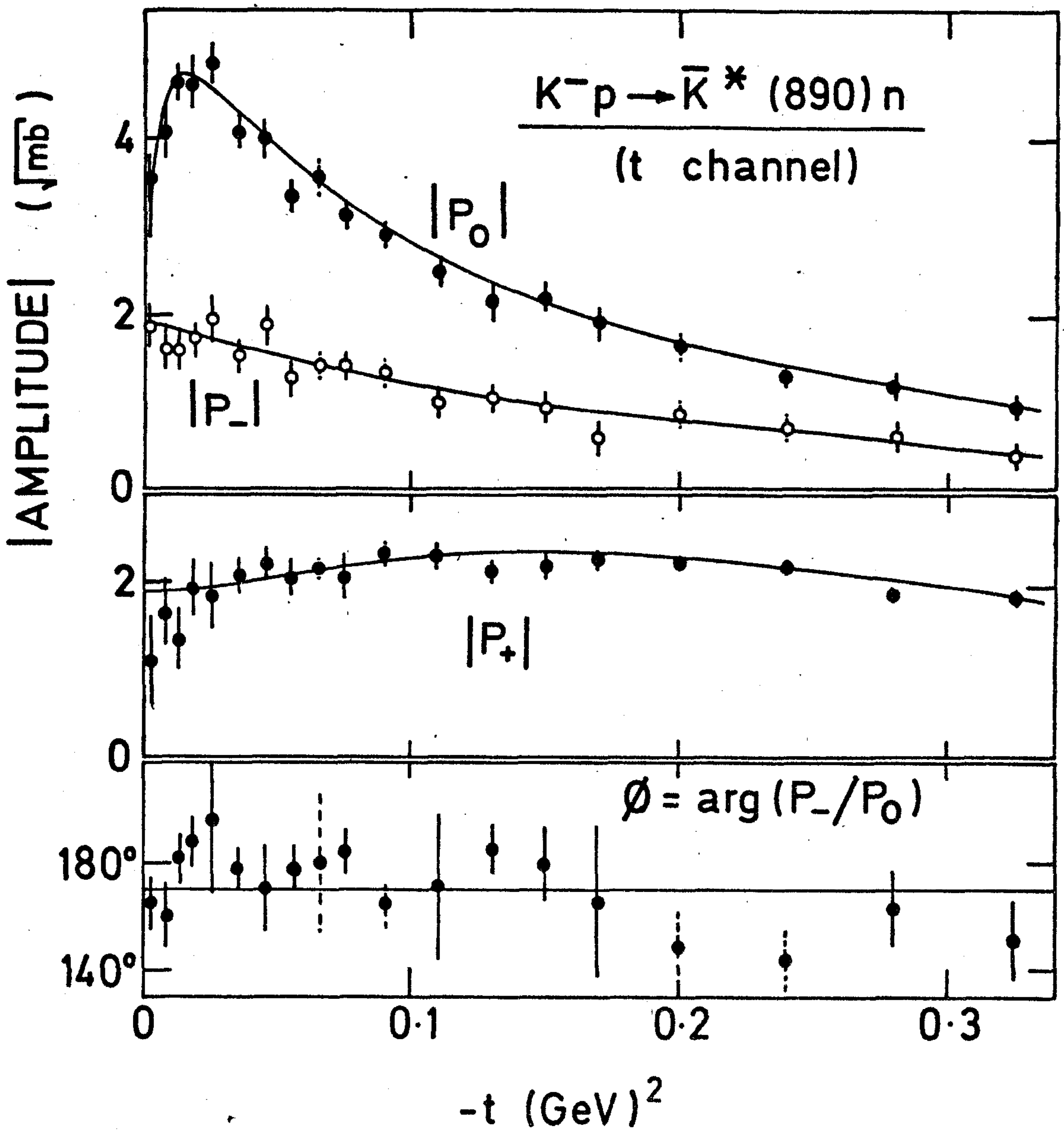
K⁻p → K̄* (890) n
(t channel)
|AMPLITUDE| ($\sqrt{mb}$)
4
2
0
|P₀|
|P₋|
2
0
|P₊|
ø = arg (P₋/P₀)
180°
140°
0
0·1
0·2
0·3
-t (GeV)²

FIG. 3

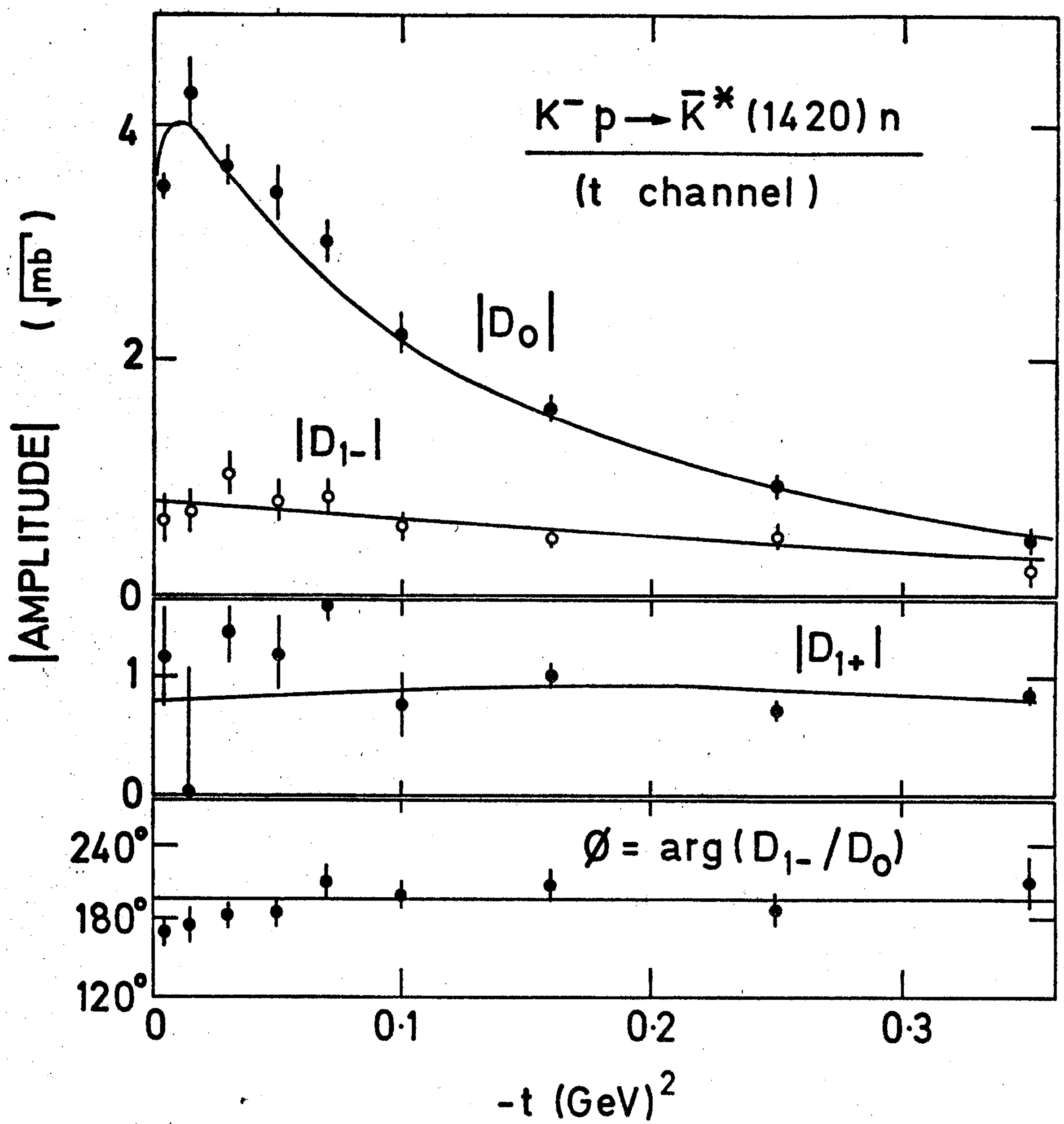

$K^- p \to \bar{K}^*(1420)\,n$
(t channel)
$|D_0|$
$|D_{1-}|$
$|D_{1+}|$
$\phi = \arg(D_{1-}/D_0)$
|AMPLITUDE| ($\sqrt{mb}$)
4
2
0
1
0
240°
180°
120°
0
0·1
0·2
0·3
-t (GeV)^2

FIG. 4